# Group Delay Measurement For Satellite Payload Testing

A.C. Newell, S.F. Gregson, P. Pelland, D. Janse van Rensburg
NSI-MI Technologies LLC,
19730 Magellan Drive,
Torrance, California, USA

***Abstract*—In this paper, we present a method for measuring antenna group delay (GD) in a planar near-field range. The technique is based on a set of three antenna pairs, measured sequentially, from which the insertion phase of the measurement system and the near-field probe can be resolved. Once these parameters are known, insertion phase for the device under test (that is to say a Tx or Rx antenna) can be measured and GD calculated as the negative frequency derivative of the insertion phase with respect to frequency. An added complexity in the case of a near-field measurement is the near-field probe is in close proximity to the device under test, does not satisfy the far-field condition. We also show that group delay can be extracted from a single near-field measurement point in the antenna's aperture plane, leading to significant test time savings. Measured results are presented and discussed.**

## I. INTRODUCTION

Equivalent Isotropically Radiated Power (EIRP), Saturating Flux Density (SFD) and Group Delay (GD) are three system level parameters often measured during the characterization of spacecraft systems. EIRP is of interest for transmitters, SFD for receivers and GD for the entire up/down link. A test methodology for EIRP and SFD was first presented in [1] and [2] and a detailed procedure presented in [3]. To date GD has only been measured under far-field (or simulated far-field) conditions. In [4], a concept for measuring GD in a planar near-field (PNF) range was described, however no methodology was included and in [5] a three-antenna method is discussed, however the treatment is limited to the far-field case. In this paper, we develop a three-antenna GD calibration procedure that is effective in the near and far-zones and examine how it varies with measurement distance.

## II. OVERVIEW OF GROUP DELAY

For a two-port linear time-invariant (LTI) system GD is defined as the negative of the rate of change of transmission phase angle with respect to frequency. Ideally, this delay should be the same for all frequency components if distortion at the output is to be avoided. When expressed mathematically the propagation group delay, defined by the Brillouin equation [6], can be stated as follows,

$$GD = -\left(\frac{d}{d\omega}\Phi_{21}\right) \tag{1}$$

Here, $\Phi_{21}$ is the insertion phase angle expressed in radians and is the argument of the forward transmission scattering coefficient, $S_{21}$. That is to say, the group delay is defined to be the negative slope of the phase response of the LTI system being considered. This can be considered to represent the delay of the envelope of the modulating signal and serves as a transfer function to characterize signal dispersion. Through an exchange of variables, and again assuming that the phase angle is expressed in radians, this can be expressed equivalently as,

$$GD(f) = -\frac{1}{2\pi}\frac{d\Phi(f)}{df} \tag{2}$$

For practical numerical cases, equation (2) can be approximated by a sided difference where the frequency step is made as small as is practical,

$$GD(f_0) \approx -\frac{1}{2\pi}\frac{\Phi(f_1)-\Phi(f_0)}{f_1-f_0} \tag{3}$$

Alternatively, and providing the frequency points are monotonic and equally spaced, a more accurate numerical derivative can be obtained by taking central differencing (with sided-differences being taken at the extremities of the data arrays),

$$GD(f_0) \approx -\frac{1}{2\pi}\frac{\Phi(f_1)-\Phi(f_{-1})}{f_1-f_{-1}} \tag{4}$$

By way of an illustration, Figure 1 contains a plot of the calculated group delay of a 0.3 m (12 inch) long section of WR90 waveguide as a function of frequency. Here, it is evident that near the waveguide cut-off, the group delay varies very rapidly with frequency. A typical open ended rectangular waveguide probe can be expected to behave broadly similarly and as such these probes, and any waveguide horns, should be used well away from their cut-off frequency.

Conversely, Figure 2 shows the group delay for a 0.127 m (5 inch) section of WR34 rectangular waveguide section across a more limited frequency span where the group delay is essentially independent of frequency, *cf.* results presented in the following section.

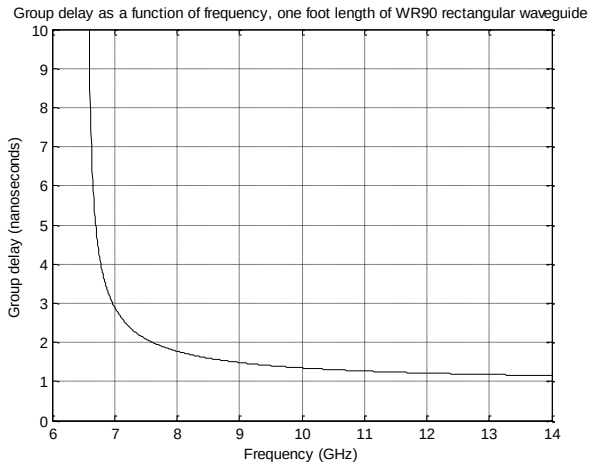


**Figure 1: Group delay shown as a function of frequency for a 0.30 m (12 inch) section of WR90 waveguide.**

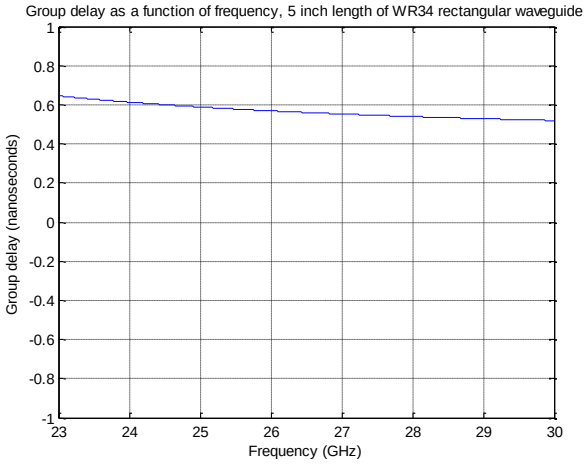


**Figure 2: Group delay of 0.127 m (5 inch) section of WR34 rectangular waveguide.**

When attempting to measure the group delay of a given test antenna it is crucial that the performance of this antenna be isolated from the other parts of the RF subsystem. These constituent parts are illustrated in Figure 3 below. In general, we can consider that the phase is measured between the two ports of the vector network analyzer (VNA). This means that in addition to the AUT, the phase change introduced by the guided wave path, the probe and the free space between that exists between the AUT and the probe, all need to be taken into account. Although the following treatment pertains specifically to planar near-field measurements, the method is far more general and could be applied to other geometries.

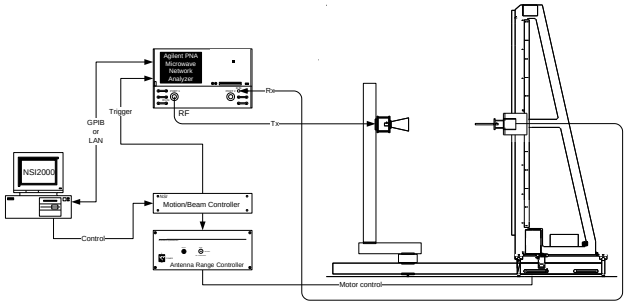


**Figure 3: RF subsystem in near-field test system showing guided wave path, AUT, probe and free space portions**

Let us assume that near-field measurements are then taken on three antenna combinations 1 & 2, 1 & 3, and 2 & 3. Here, Antenna 1 is taken to be the AUT, Antennas 2 and 3 are assumed to be non-identical antennas. Thus, (assuming that the free space phase change has been compensated for within the near-field to far-field transform) the measured far-field phase can be expressed as,

$$\phi_1 + \phi_2 + \phi_B = \phi_{1,2} \tag{5}$$

Here, $\phi_1$ is the transmission phase through the $T_x$ antenna, $\phi_2$ is the transmission phase through the $R_x$ antenna, $\phi_B$ is the transmission phase through the guided wave portion of the RF subsystem and $\phi_{1,2}$ is the measured phase through the system. Here, we assume that we can measure $\phi_B$ by connecting the cable to the $T_x$ and $R_x$ antennas together and measuring this bypass phase. As a part of this measurement, we will need to calibrate out, or ignore, the insertion phase of any RF adapters that are needed to allow the RF cables to be connected together. Thus, three relationships for the three measurements can be expressed as,

$$\phi_1 + \phi_2 = \phi_{1,2} - \phi_B \tag{6}$$

$$\phi_1 + \phi_3 = \phi_{1,3} - \phi_B \tag{7}$$

$$\phi_2 + \phi_3 = \phi_{2,3} - \phi_B \tag{8}$$

When rearranging these three equations the transmission phases of the individual antennas can be obtained and expressed in terms of the measured parameters similar to what is done during the three-antenna gain measurement method [7],

$$\phi_1 = \frac{1}{2}\left[\phi_{1,2} + \phi_{1,3} - \phi_{2,3} - \phi_B\right] \tag{9}$$

$$\phi_2 = \frac{1}{2}\left[\phi_{1,2} + \phi_{2,3} - \phi_{1,3} - \phi_B\right] \tag{10}$$

$$\phi_3 = \frac{1}{2}\left[\phi_{1,3} + \phi_{2,3} - \phi_{1,2} - \phi_B\right] \tag{11}$$

Thus, the individual phases can be obtained from the three separate antenna measurements without a priori knowledge. The close proximity between the AUT and the probe means that this technique can be susceptible to errors resulting from AUT to probe multiple reflections. It is important to note that

the range of phase angles is limited to modulo π which is *half* the ordinary phase range. Thus, when evaluating equations 9 - 11 the resulting phases must be wrapped back into modulo π phase range. However, before the group delay can be computed the phase needs "unwrapping" by changing absolute phase jumps greater than or equal to π to their complimentary angle. Then, the group-delay can be computed using the usual formula. Failure to do this properly results in discontinuities being encountered within the resulting calculated group delay.

In general, in the far-field, the transmission phase is a function of the orientation of the respective antennas and the position of those antennas when they were tested within the range. However, if we limit ourselves to considering the θ = ϕ = 0° boresight point and we assume that any correction for the offset of the AUTs from the origin of the measurement coordinate system is implemented during the near-field to far-field transformation [7], which is usually the case, then then equations (9) – (11) remain valid.

## III. Three-Antenna Group Delay Measurement Setup

The method presented above was used to compute the group delay of three antennas; a center fed parabolic reflector antenna with diameter *D*, a pyramidal horn and an open ended rectangular waveguide probe. The separation, sampling density and physical location of the antenna under test did not necessarily remain static between the three sets of measurements. The near-field amplitude distribution of the parabolic reflector is shown in Figure 4. The reflector's feed produces considerable blockage at the center of the circular aperture. This is important to note and should be considered when computing group delay directly from the near-field phase response as signal to noise ratio will be limited in this region.

Planar near-field measurements were taken for the three combinations across the frequency range that spanned 23 to 30 GHz. Additionally, a bypass measurement was also made that was intended to allow the phase of the guided wave path of the RF subsystem to be extracted from the measurements. Unfortunately, it was found that this data contained artefacts from impedance mismatch induced multiple reflections which were undesirable. As it is possible to transform S-parameter data to the time domain from the frequency domain using the time-frequency Fourier relationship [7], it was possible to suppress these effects. It is well known that the time-domain signal can be obtained from the frequency domain data using an inverse Fourier transform using,

$$s_{21}(t) = \int S_{21}(f) e^{j2\pi ft} df \qquad (12)$$

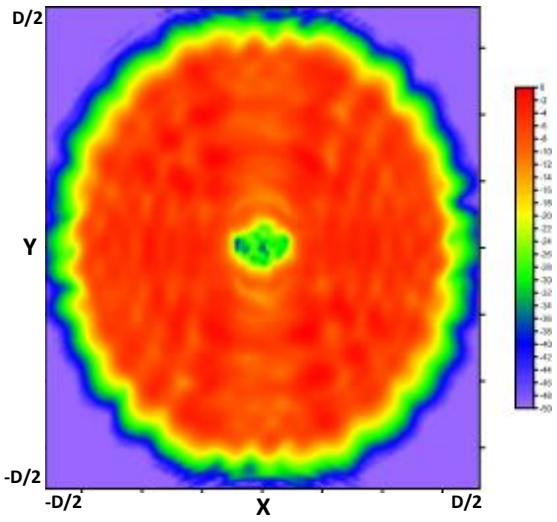


**Figure 4: Near-field amplitude distribution of center fed parabolic reflector antenna.**

Conversely, the transform from the time-domain to the frequency-domain can be expressed as,

$$S_{21}(f) = \int s_{21}(t) e^{-j2\pi ft} dt \qquad (13)$$

When the bypass measurement (transmission) S-parameter data is transformed to the time domain and the amplitude is plotted as a function of time in logarithmic form, we obtain the time domain result as shown in Figure 5 below.

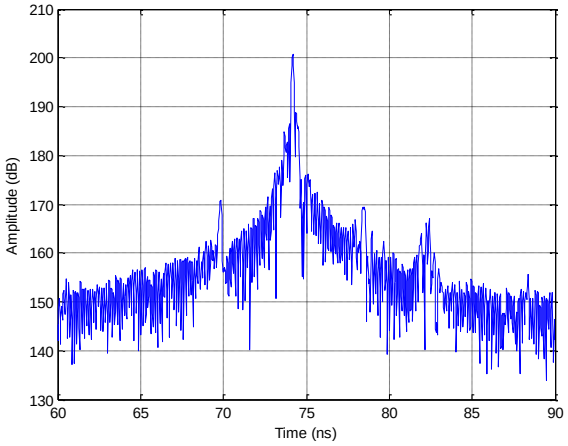


**Figure 5: Time domain plot of $S_{21}$ showing the time taken for the signal to propagate through the RF system.**

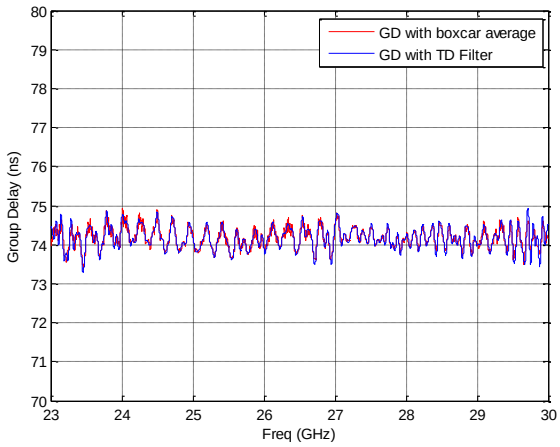


**Figure 6: Group delay plotted as a function of frequency of bypass measurement.**

Figure 5 shows the transmission scattering coefficient plotted as a function of time. Here it is clear that the largest signal takes approximately 74 ns to propagate through the network. However, it is also evident that there is a great deal of spurious signals that can be seen to take significantly longer to propagate through the system. These can be filtered out with the remaining signal being transformed back to the frequency domain providing reliable calibration data for the three-antenna method. Clearly, the group delay can be computed directly from the unwrapped phase function as described above and is shown in Figure 6. Here, a 41 point "boxcar" average was applied to the GD data so as to be able to reveal the underlying function. The GD data was initially computed at 7001 points spanning 23 to 30 GHz where the 7001 points corresponded to the number of $S_{21}$ samples that were taken in the finely sampled "bypass" measurement. This was compared to the equivalent result as obtained by applying a band-pass filter to the time-domain data, which is shown as the blue trace.

## IV. Preliminary Results

Figure 7 below presents the group delay as calculated using the three-antenna method with the phase values being taken from the $\theta = \phi = 0°$ far-field peaks of the three combination measurements using the technique described in Section II. Note that negative group delay is not implying superluminal behavior. If one considers wave propagation over a physical distance $R$, this translates to a phase change of $-k_0R$, where $k_0$ is the free-space wavenumber. Assuming that the medium is non-dispersive, this implies a linearly decreasing phase change as a function of increasing frequency. Taking the negative derivative of this linear function, leads to a constant positive group delay. This observation leads one to conclude that a negative GD corresponds to a positively sloped phase function versus an increase in frequency, which implies slower wave propagation velocities at higher frequencies – the opposite of what one would observe in rectangular waveguide, for instance. Nevertheless, this is a characteristic that could be observed when dealing with complex radiating structures. Here, the pyramidal horn and open ended waveguide probe both behave like waveguide above cutoff, as one would expect and align with the result shown above in Figure 2.

By way of a comparison, this calculation was repeated only here the phases were extracted from a single point within the parabolic reflector's aperture plane, $z = 0$. Here, the $x = 0$, $y = 0.25D$, $z = 0$ point was used and can be found presented in Figure 8. The particular $(x,y)$ point was selected as it sits outside of the near-field blockage region shown in Figure 4 above. Here, $D$ refers to the diameter of the circular reflector antenna. The phase response at the aperture plane is extracted using the standard plane-to-plane transform technique [7],

$$F(k_x, k_y, z=0) = \int_{-\infty}^{\infty}\int_{-\infty}^{\infty} E(x, y, z=0) e^{j(k_x x + k_y y)} dx dy \tag{14}$$

Whereupon,

$$E(x, y, z) = \frac{1}{4\pi^2}\int_{-\infty}^{\infty}\int_{-\infty}^{\infty} F(k_x, k_y, z=0) e^{-j(k_x x + k_y y + k_z z)} dk_x dk_y \tag{15}$$

Thus, the field over one plane in space can be used to calculate the equivalently polarized field over the surface of another, parallel plane displaced by a distance $z$ in the $z$-axis. As only the propagating near-field is sampled the limits of integration in (15) can be collapsed to,

$$k_x^2 + k_y^2 \le k_0^2 \tag{16}$$

Please note that the purpose of using the plane-to-plane transform was to allow the GD calculation to be examined at a variety of different points in space as opposed to being a fundamental part of the GD calculation.

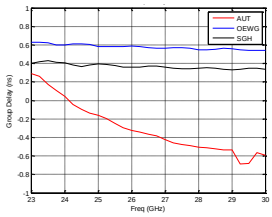


**Figure 7: Group delay of AUT, SGH & probe calculated in the far-field.**

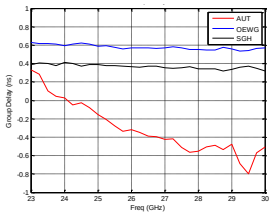


**Figure 8: Group delay of AUT, SGH & probe calculated in aperture plane at x = 0, y = 025D, z = 0.**

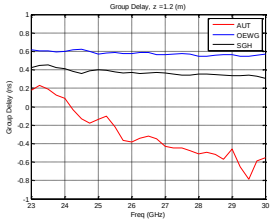


**Figure 9: Group delay of AUT, SGH & probe calculated at x = 0, y = 0.25D, z = D.**

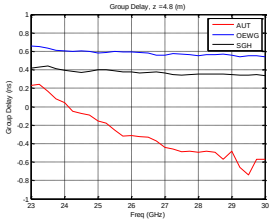


**Figure 10: Group delay of AUT, SGH & probe calculated at z = 4D.**

The group delay was calculated again at $z = D$ and $z = 4D$ and is plotted in Figure 9 and Figure 10, respectively. The results derived from the near-field phase show encouraging similarities to the result derived from the far-field. The plane-to-plane transform was used as it provides the most reliable near-field data. However, it should be noted that one can also use the phase from the near-field measurement plane to eliminate the extra step of the plane-to-plane transform.

These calculations can be repeated using other $x$, $y$ positions in the near-field with very similar results being obtained providing the signal to noise ratio is good. It is possible to improve the results by averaging across a number of different near-field points and examples of this can be found in Figures 11 and 12 below. Here, for example, 101 data points in the near-field region were averaged with care taken to ensure points in the blockage region were excluded. These results show encouraging agreement with the far-field result presented in Figure 7 above.

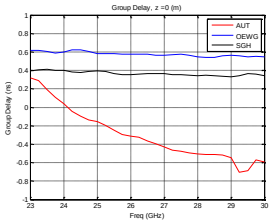


**Figure 11: Group delay of AUT, SGH & probe calculated in the aperture plane, $z = 0$.**

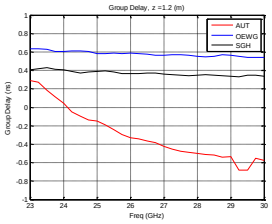


**Figure 12: Group delay of AUT, SGH & probe calculated at $z = D$.**

The averaging that is obtained by combining results from a number of points selected at random across the measurement plane is evident. These results provide very good agreement with the result obtained from examining the far-field boresight phase, *cf.* Figure 7 above. This is expected as, for the planar case, the near-field to far-field transform for the $\theta = \phi = 0°$ point equates to a vector sum although this would not be true for other far-field directions.

## V. Simplified Group Delay Measurement

The treatment presented above allows one to determine the group delay of an antenna in a very general manner. Although the results of the previous section demonstrate that it is possible to determine antenna GD from measurements made in the near-field without the requirement for taking complex two-dimensional near-field scans, it does still necessitate the measurement of three pairs of antennas, which is time consuming and therefore ultimately undesirable. However, for the case presented above, it is evident that providing the GD is computed at frequencies that are not too close to the waveguide band crossings, that is to say well away from the cut-off of the fundamental $TE_{10}$ mode, then the GD is comparatively insensitive to frequency. Furthermore, it may also be possible to select probes that further minimize the amount of GD, *e.g.* by reducing the length of the open ended rectangular waveguide (OEWG) probe or alternatively, by selecting an alternative GD optimized probe.

To illustrate this further, Figure 13 below presents a comparison of measured near-field phase and calculated far-field phase. Here, the similarity between the two traces is evident which suggests that the GD that is calculated from this phase function will be in similarly encouraging agreement. Please be aware that as GD is obtained from the slope of the phase function the constant offset between the traces is unimportant. This is an important result as, in contract to those results presented in the previous section; the three-antenna measurement method was *not* used.

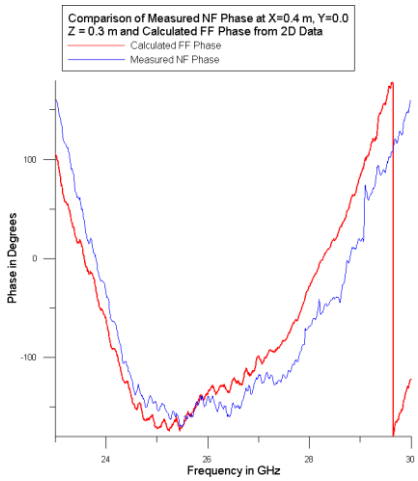


**Figure 13: Comparison of measured near-field phase and calculated far-field phase.**

The group delay measurement technique presented above using the three-antenna technique and the bypass measurement illustrates that we can account for all the details in the measurement if necessary. However, a user will not necessarily want to invest the time and resources necessary to perform the full three-antenna measurement every time they measure GD with the result shown in Figure 13 suggesting that the GD of the transmission line and the probe are potentially small enough that in a practical measurement they may be neglected.

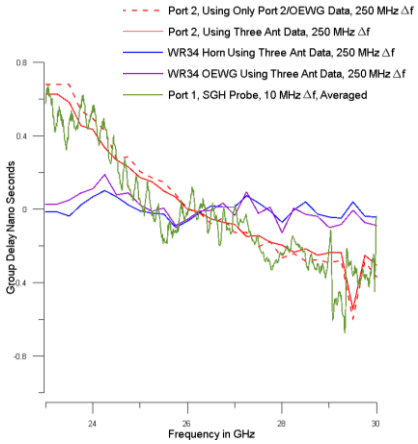


**Figure 14: Comparison of GD delay of AUT and SGH calculated using different approaches.**

So that this possibility could be further explored, the GD was computed using the three-antenna method and using only

the AUT-to-probe near-field data. Figure 14 above shows a comparison of the GD as calculated using the three-antenna method and the transmission phase as obtained from a conventional measurement between AUT and probe. It is clear that the results are in good agreement, noise aside, for both the complex reflector antenna and the comparatively simple pyramidal horn suggesting that the GD of the probe is small, *cf.* Figure 2 above, and may be ignored in many circumstances. During the preparation of this result, in order to simplify the processing, a linear phase term was removed from the measured phase and explains the difference in the normalization of the absolute GD value when compared to the result shown above in Section IV. Removal of linear term is not required for group delay calculations. The liner term is removed to examine the phase versus frequency graphically to examine the detail within the data. Removing linear term illustrates presence of high frequency variations that produce "noise" in group delay results which can be mitigated through time-gating or with the use of a boxcar average, as illustrated above in section III, *cf.* Figure 6.

By way of a further verification, an additional GD measurement was made at X-band. As with the Ka-band test discussed above, the GD was computed at different positions in the near-field. These GD results were compared with the GD result that was obtained from using the far-field boresight point and the difference can be seen plotted below in Figure 15. Here, it is clear that the difference is very small and is independent of frequency.

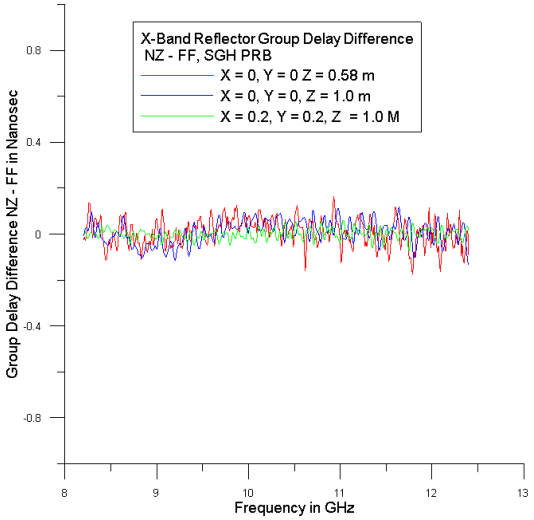


**Figure 15: Plot showing difference between GD calculated in the far-field and GD calculated at different positions in the near-field.**

## VI. Summary and Conclusions

This paper has presented the development and preliminary validation of a three-antenna measurement technique for determining the group delay of a given antenna. This paper then shows that this method can be used in the near-field providing the point chosen has good signal to noise ratio. It is also used to confirm that it is possible, in certain cases, to use a simpler method involving just the AUT and a near-field probe. Thus, this paper has shown that it is very likely that the group delay measurements can be made between the probe and the AUT at the same *z* distance that was used for the conventional planar near-field measurements using the near-field phase that was obtained during the regular antenna pattern measurement. Furthermore, the comparisons shown above, and others not shows due to practical limitations of space, confirm that there is very little difference between group delay calculated using just the derivative of the measured near-field phase at any high amplitude point within the near-field data set and the group delay derived from calculating the derivative of the boresight far-field phase as obtained from using all the near-field data. Although this is perhaps an initially surprising result, it is worth keeping in mind that GD is neither a near-field nor a far-field property. Like frequency bandwidth, it is a property of the antenna that is in principal independent of the location of the reference point. Thus, providing the slope of the measured transmission phase is recovered and treated correctly, the ensuing GD should be reliable. Hence, it may also be possible to measure group delay by placing a suitable probe at a single point in the near-field and observing the distortion of the pulse transmitted from the probe. Consequently, the planned future work is to include obtaining experimental verification of this approach. Although these conclusions are preliminary, they are based on the measurement and analysis of two different antennas operating at different frequencies, these conclusions align with the findings reported by other workers and will be followed up with further verified with additional measurement and analysis.

## References


[1] A. C. Newell, R. D. Ward and E. J. McFarlane, "Gain and power parameter measurements using planar near-field techniques", IEEE Trans. Antennas &Propagat, Vol 36, No. 6, June 1988.

[2] A. C. Newell, "Planar near-field antenna measurements", NIST EM Fields Division Report, Boulder, CO, March 1994.

[3] D. Janse van Rensburg and K. Haner, "EIRP & SFD Measurement methodology for planar near-field antenna ranges", Antenna Measurement Techniques Association Conference, October 2014.

[4] C. H. Schmidt, J. Migl, A. Geise and H. Steiner, "Comparison of payload applications in near field and compact range facilities", Antenna Measurement Techniques Association Conference, October 2015.

[5] A. Frandsen, D. W. Hess, S. Pivnenko and O. Breinbjerg, "An augmented three-antenna probe calibration technique for measuring probe insertion phase", Antenna Measurement Techniques Association Conference, October 2003.

[6] L. Brillouin, "Wave Propagation and Group Velocity", Academic Press, New York, 1960.

[7] C.G. Parini, S.F. Gregson, J. McCormick, D. Janse van Rensburg "Theory and Practice of Modern Antenna Range Measurements", IET Press, 2014, ISBN 978-1-84919-560-7.